JACS
JOURNAL OF THE AMERICAN CHEMICAL SOCIETY
Communication
pubs.acs.org/JACS

Iron(III)-Based Metal–Organic Frameworks As Visible Light Photocatalysts

Katrien G. M. Laurier,[†] Frederik Vermoortele,[‡] Rob Ameloot,[‡] Dirk E. De Vos,[‡] Johan Hofkens,[†] and Maarten B. J. Roeffaers*[,†,‡]

[†]Department of Chemistry, KU Leuven, Celestijnenlaan 200F, B-3001 Heverlee, Belgium
[‡]Department of Microbial and Molecular Systems, KU Leuven, Kasteelpark Arenberg 23, B-3001 Heverlee, Belgium

Supporting Information

ABSTRACT: Herein, a new group of visible light photocatalysts is described. Iron(III) oxides could be promising visible light photocatalysts because of their small band gap enabling visible light excitation. However, the high electron–hole recombination rate limits the yield of highly oxidizing species. This can be overcome by reducing the particle dimensions. In this study, metal–organic frameworks (MOFs), containing Fe_3-μ_3-oxo clusters, are proposed as visible light photocatalysts. Their photocatalytic performance is tested and proven via the degradation of Rhodamine 6G in aqueous solution. For the first time, the remarkable photocatalytic efficiency of such Fe(III)-based MOFs under visible light illumination (350 up to 850 nm) is shown.

Photocatalysis is a proven, useful approach to solve environmental issues such as air and water pollution. Since the pioneering work of Fujishima and Honda in 1972, much research has focused on semiconductor-based photocatalysts and photocatalytic processes using titanium dioxide (TiO_2).[1] Although TiO_2 is stable, reactive, and available at relatively low cost, it only absorbs ultraviolet (UV) light because of its large band gap. This has stimulated researchers to develop novel materials with a reduced band gap to enhance the response to the more abundant visible light photons. Doping TiO_2 with organic or inorganic compounds to enhance the optical response to the visible light is a popular strategy.[2,3] Nevertheless, the resulting materials often have limited stability or suffer from an increase in charge carrier recombination which is detrimental to the catalytic performance. Therefore, a number of semiconductors, often oxides, with a visible light response, such as WO_3,[4] $BiVO_4$,[5] and Fe_2O_3,[6] have been evaluated as alternatives. Based on its abundance, stability, nontoxic nature, and much smaller band gap, iron(III) oxide in particular is a promising candidate for the development of efficient solar photocatalysts. However, iron(III) oxide has one significant drawback: its photocatalytic performance is limited by the high recombination rate of the photogenerated charge carriers.[7] To minimize electron–hole recombination, hydrogen peroxide or Fe^{3+}-ions have been proposed as sacrificial agents to scavenge the photoelectrons.[8,9] Alternatively, the fast recombination can be overcome by downsizing the photocatalytic particles, thus enabling the charge carriers to effectively reach the reactants adsorbed at the surface.[10,11] In relation to the latter approach, metal–organic frameworks (MOFs) are very interesting materials. MOFs are porous, crystalline inorganic/organic solids built up from metal(oxide) clusters interconnected by polydentate organic linkers.[12−14] For example, MOFs can consist of Fe(III)-oxide clusters, linked together in three dimensions by organic linkers. Several MOFs are known that contain Fe_3-μ_3-oxo clusters as a structural motif, with a great variety in topology and pore sizes depending on the organic linker and preparation conditions used. Thanks to the small size of the Fe_3-μ_3-oxo cluster, limited recombination and thus a high photocatalytic activity could be expected in such MOFs. Research on the photocatalytic properties of MOFs has started recently. The group of García has reported UV photocatalytic activity in MOF-5.[15,16] Titanium and zirconium based MOFs, respectively MIL-125 and UiO-66, have also been shown to be UV photoactive.[17,18] However, because of the lack of visible light response, these materials would show limited efficiency under solar illumination. An opportunity to tune these optical properties lies in the modification of the organic linkers, yielding an elevated visible light response. In this context, Gascon et al. reported on the effect of modifying the linker properties to lower the overall band gap of MOF-5.[19] Moreover, visible light photocatalytic activity can be introduced via linker substitution with an amino group.[18,20,21]

In this study, we use small iron(III) oxide clusters as the inorganic nodes in hybrid photocatalytic materials. These clusters show inherent absorbance of visible light and are efficiently separated from one another due to confinement in a metal–organic framework. Screening of their activity was done via the photocatalytic degradation of an organic dye (Rhodamine 6G) in an aqueous solution under visible light illumination. The obtained performances were compared to those of the commercial titanium dioxide photocatalyst P25, obtained from Evonik, and an iron(III) oxide (Fe_2O_3) nanopowder supplied by Sigma-Aldrich. One iron(III)-based metal–organic framework was also commercially obtained and will be referred to by its commercial name, Basolite F300. The other iron(III)-based MOFs were synthesized according to literature procedures: MIL-100(Fe),[22] amino-substituted MIL-101(Fe),[23] MIL-88B(Fe), and amino-substituted MIL-88B-(Fe).[24,25] Furthermore, an amorphous gel with a similar

Received: May 21, 2013
Published: September 9, 2013

   dx.doi.org/10.1021/ja405086e | J. Am. Chem. Soc. 2013, 135, 14488−14491

composition as amino-substituted MIL-101(Fe) was synthesized and will be referred to as Fe(III)-aminogel.[26] The chemical composition of each of the used MOF photocatalysts is listed in the Supporting Information (SI), section 2.1.

The optical response of the photocatalytic materials was investigated by diffuse-reflectance UV−vis spectroscopy. Figure 1 represents the reflection spectra of the studied photocatalysts.

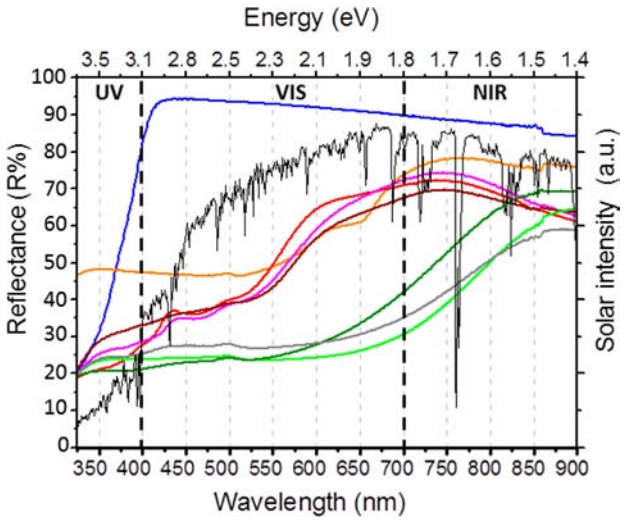

Figure 1. Diffuse reflectance spectra of P25 (blue), Fe_2O_3 (gray), MIL-100(Fe) (orange), Basolite F300 (red), MIL-88B(Fe) (pink), amino-substituted MIL-88B(Fe) (dark red), amino-substituted MIL-101(Fe) (light green), and Fe(III)-aminogel (green). The black curve represents the relative solar spectrum (ASTM G173-03).

From these spectra it is obvious that all of the iron(III)-based solids in this study have a clear optical response in the visible light region. This is in contrast with the commercial UV active titanium dioxide sample, P25 (blue curve). The Fe(III)-MOFs can absorb photons with energy equal or higher than their HOMO−LUMO gap, comparable to the band gap of traditional semiconductor based photocatalysts, such as TiO_2. The maximum wavelength that can be absorbed by the different materials in this study ranges from 400 nm for P25 up to about 825 nm for the amino-substituted MIL-88B(Fe) and Fe(III)-aminogel. The values are listed in the SI (section 2.3).

To assess the photocatalytic activity of these iron(III)-based solids, the degradation of a 100 μM Rhodamine 6G (Rh6G) aqueous solution was selected, as its degradation can easily and quantitatively be monitored via its fluorescence intensity. Furthermore, Rh6G was chosen because of its high stability against spontaneous photobleaching in the absence of a photocatalyst. Before the photocatalytic assays were started, the samples were stirred in the dark in order to reach the adsorption equilibrium. The photocatalytic wavelength-dependent screening experiments were performed by illuminating the samples with monochromatic light. To map the activity of a certain material throughout the UV and visible light spectrum, the monochromatic excitation light (1−7 mW) was varied between experiments (350 ± 5 nm, 450 ± 5 nm, 550 ± 5 nm, 650 ± 5 nm, 750 ± 5 nm, and 850 ± 5 nm). While illuminating the sample, the fluorescence of Rh6G near the emission maximum, at 570 nm, was monitored for 1 h. At wavelengths where direct excitation to measure the fluorescence was not possible (650, 750, 850 nm), the emission of Rh6G was measured every 4 min to monitor its degradation. Typically, the fluorescence of Rh6G shows an exponential decay in time, which can be expected because of the formation of side products which compete for photocatalytic degradation (e.g., Figure 2). These decay curves allow us to quantify the Rh6G degradation.

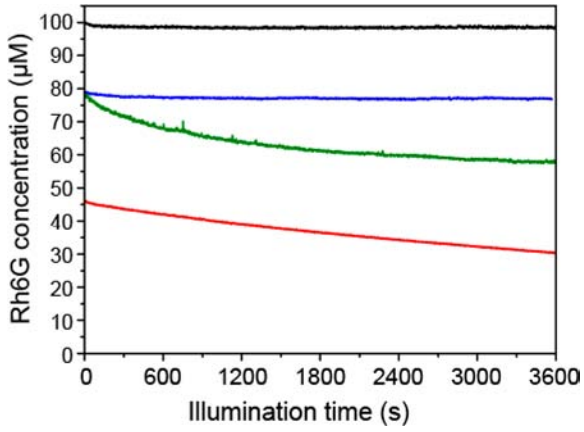

Figure 2. Visible light photocatalytic degradation of Rhodamine 6G when illuminated at 550 nm as a function of time: without photocatalyst (black) and in the presence of P25 (blue), Basolite F300 (red), and Fe(III)-aminogel (green).

The fluorescence emission of the photostable Rh6G in the absence of a photocatalyst (Figure 2, black) shows only very minor photobleaching. Nonetheless, the photocatalytic degradation is always corrected for this small amount of photobleaching. It was also observed that after stirring in the dark the samples adsorb part of the Rh6G molecules, which results in a lower starting concentration of the Rh6G solution for the photocatalytic reactions. No sorption or intracrystalline diffusion of Rhodamine 6G in the used MOFs is expected because of the typical pore sizes of the materials used. Hence, dye adsorption will only occur at the outer surface of the MOF particles.

As expected, the commercial TiO_2 photocatalyst P25 shows no photocatalytic degradation of Rh6G when illuminated with 550 nm. However, similar visible light stimulation of Basolite F300 and Fe(III)-aminogel results in a considerable degradation of Rh6G in aqueous solution. The photocatalytic Rh6G degradation rates, measured as a function of the illumination wavelength and averaged over 1 h, are summarized in Figure 3. To relate these results to photocatalytic activities under solar illumination the data are corrected for the number of photons at the different wavelengths illuminating the sample compared to the relative number of photons present in the solar spectrum (ASTM G173-03). Furthermore, the data are normalized for the number of metal atoms present in each photocatalyst. The photocatalytic degradation can be related to different pathways. Next to the direct photocatalytic degradation of Rhodamine 6G molecules adsorbed at the photocatalyst, photogenerated electron−hole pairs can generate highly oxidative species such as hydroxyl radicals and superoxide anions. These mobile radicals will indirectly degrade the Rhodamine 6G molecules in the surrounding solution.

Figure 3 clearly shows remarkably high visible light photocatalytic activity for most iron(III) oxide based MOFs compared to the UV-responsive P25 reference catalyst. For the commercial Fe_2O_3 nanopowder, no photocatalytic activity could be observed for the system under study, which indicates

dx.doi.org/10.1021/ja405086e | J. Am. Chem. Soc. 2013, 135, 14488−14491

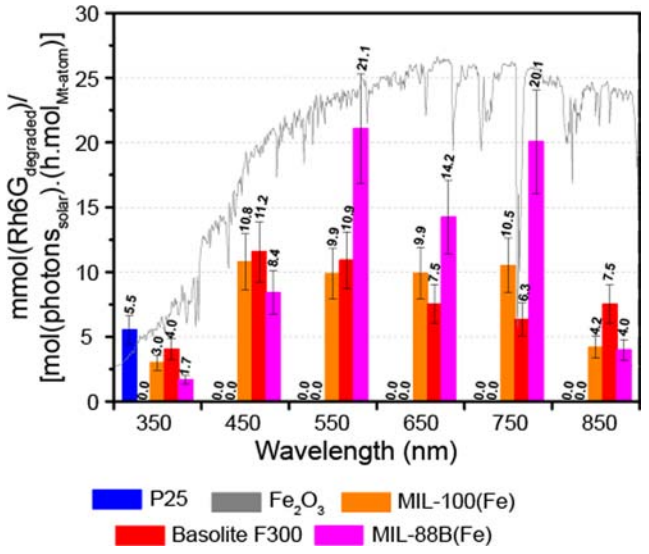

Figure 3. Photocatalytic Rh6G degradation (normalized per metal atom) at selected wavelengths. The relative solar spectrum (ASTM G173-03) is shown in the background.

that fast electron−hole recombination is the dominant process under these experimental conditions.[7] The different Fe(III)-MOF samples all display clear visible light photocatalytic activity. The highest overall visible light photocatalytic activity was measured for the metal−organic framework MIL-88B(Fe). MIL-88B(Fe) is composed of Fe_3-μ_3-oxo clusters interconnected by oxidation-stable terephthalate linkers resulting in a 3D network. Since the linker does not absorb any visible light, the Fe_3-μ_3-oxo cluster in the MOF is responsible for the visible light absorption and the associated photocatalytic activity. Therefore, homogeneous iron(III) acetate clusters were investigated as a possible reference.[27] However, no photocatalytic activity was measured under similar conditions. This could be a result of the low stability of such clusters in the presence of water.[28] Structuring these clusters in the extended network of a MOF results in higher cluster stability. Another metal−organic framework consisting of the same clusters, but with a different linker and topology, is MIL-100(Fe). In this MOF, the clusters are interconnected by trimesic acid in three dimensions. MIL-100(Fe) also exhibits visible light photocatalytic activity; however, the photocatalytic activity at green and red wavelengths is lower than that of MIL-88B(Fe). This indicates that not only the cluster but also the linker and the framework topology of the MOF determine the overall photocatalytic activity. As stated in the introduction, iron oxide clusters packed too close to each other (like in Fe_2O_3) are disadvantageous regarding recombination. Furthermore, a commercial MOF, Basolite F300, was measured. Although Basolite F300 and MIL-100(Fe) have a similar chemical composition, differences in crystallinity (Basolite F300 reveal poor crystallinity compared to MIL-100(Fe)) could result in differences in (photo)catalytic performance.[29] However, the differences in photocatalytic activities obtained in this study are within the margin of error. From these results, it is concluded that high crystallinity is not necessarily a requirement to obtain good photocatalytic activity. We expect that the stability of the local order of the Fe_3-μ_3-oxo clusters is crucial to generate reasonable photocatalytic activity. Moreover, the diffusion of the reactive species (vide supra) may be hindered by a long-range order. For a good Fe(III)-MOF photocatalyst, a balance between local and long-range order in the photocatalytic particles is expected to be beneficial.

Linker modification has been proven to be beneficial for UV-active MOF photocatalysts based on titania or zirconia clusters regarding visible light photocatalytic activity in the blue part of the solar spectrum.[18,20,21] From the DRS measurements it can be concluded that the amino-substituted Fe(III)-MOF materials show a higher optical response in the visible light region compared to similar MOFs with nonsubstituted linkers. The influence of this enhanced visible light absorption on the visible light photocatalytic activity was investigated by testing amino-substituted MIL-88B(Fe) and amino-substituted MIL-101(Fe) (Figure 4). Both crystalline structures consist of the above-mentioned Fe_3-μ_3-oxo cluster interconnected by amino-terephthalic acid.

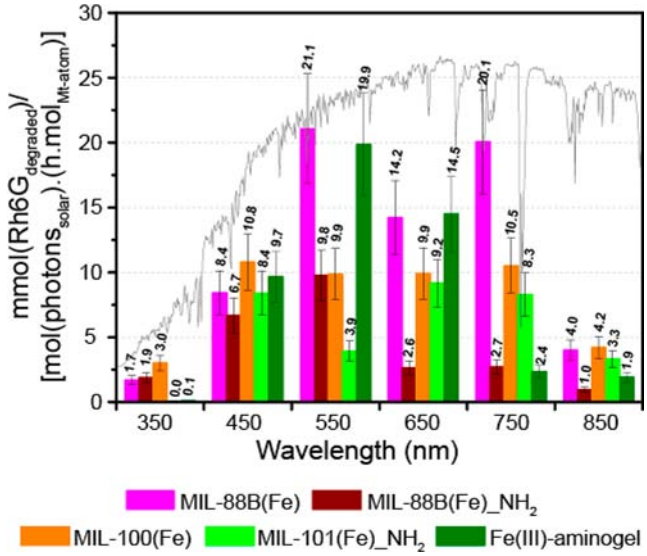

Figure 4. Photocatalytic Rh6G degradation (normalized per metal atom) at selected wavelengths. The relative solar spectrum (ASTM G173-03) is shown in the background.

In contrast to what was expected, amino-substituted MIL-88B(Fe) does not display higher visible light photocatalytic activity compared to the unsubstituted MIL-88B(Fe); its activity is in general even lower than that of MIL-88B(Fe). The same trend was observed for amino-substituted MIL-101(Fe). This observation indicates that the amount of light absorption is not directly related to the photocatalytic activity. In general, molecular interactions and dynamics in the photocatalyst influence the activity, which in turn will be influenced by linker substitution. However, an amorphous gel with the same chemical composition of amino-substituted MIL-101(Fe), namely Fe(III)-aminogel, displayed higher visible light photocatalytic activity compared to its crystalline analogue amino-substituted MIL-101(Fe). This further supports our assumption that crystallinity is not essential for a good iron(III)-based photocatalyst. Moreover, it indicates that an amorphous morphology with, however, a local order around the Fe_3-μ_3-oxo clusters may be favorable under certain conditions.

For applications of heterogeneous (photo)catalysis, it is important that the photocatalytic material is stable under the experimental conditions. The stability of the solid photocatalytic MOFs used, under the harsh conditions of the

dx.doi.org/10.1021/ja405086e | J. Am. Chem. Soc. 2013, 135, 14488−14491

photocatalytic experiments, was examined by X-ray diffraction after 24 h of UV illumination (11 mW) and stirring in a temperature-controlled photoreactor. The diffractograms of MIL-100(Fe), MIL-88B(Fe), and amino-substituted MIL-88B(Fe) show that the crystallinity of these materials is reasonably maintained (Figure S2), resulting in the assumption of a stable structure. However, for amino-substituted MIL-101(Fe) a loss of crystallinity was observed, showing lower stability in comparison with the other investigated MOFs. In addition, since preservation of crystallinity is not definitive proof for stable materials, the dye solution was also investigated with an element analysis (ICP-AES; see SI, section 2.4.1) after reaction. From these tests we can conclude that negligible iron leakage (<0.3%) occurred during all photocatalytic experiments.

In conclusion, Rhodamine 6G was successfully photocatalytically degraded under visible light illumination with different iron(III)-based metal−organic frameworks which consist of Fe_3-μ_3-oxo clusters. It was observed that crystallinity over extended length scales is not required to yield an effective photocatalyst, as the amorphous materials, with only a local order around the Fe_3-μ_3-oxo clusters (Basolite F300 and Fe(III)-aminogel), also show significant photocatalytic activity. In the case of the Fe(III)-based MOFs in this study, amino-substitution of the linker did not result in enhanced photocatalytic activity. Further development of this new class of visible light photocatalysts will require a better understanding of the photochemical mechanisms in Fe(III)-MOF materials and the crucial structural parameters controlling their photocatalytic activity.

■ ASSOCIATED CONTENT

Supporting Information

Characterization methods, properties of photocatalytic materials (chemical composition, diffractograms of synthesized photocatalysts, HOMO−LUMO gap determination, stability measurements), and photocatalytic screening measurements (procedure, illumination power spectrofluorimeter). This material is available free of charge via the Internet at http://pubs.acs.org.

■ AUTHOR INFORMATION

Corresponding Author

maarten.roeffaers@biw.kuleuven.be

Notes

The authors declare no competing financial interest.

■ ACKNOWLEDGMENTS

The authors thank Nick Duinslaeger and Kris Vandezande for helping with the experimental work. For financial support, the authors thank the Flemish government (Methusalem funding – CASAS METH/08/04), the Federal Science Policy of Belgium (IAP-PAI P7/05 "Functional Supramolecular Systems"), and the 'Fonds voor Wetenschappelijk Onderzoek' (Grants G.A035.12, G0197.11). The research leading to these results has received funding from the European Union's Seventh Framework Program (FP7/2007-2013 under Grant Agreement No. 312184).

■ REFERENCES

(1) Fujishima, A.; Honda, K. *Nature* **1972**, *238*, 37.
(2) Rehman, S.; Ullah, R.; Butt, A. M.; Gohar, N. D. *J. Hazard. Mater.* **2009**, *170*, 560.
(3) Asahi, R.; Morikawa, T.; Ohwaki, T.; Aoki, K.; Taga, Y. *Science* **2001**, *293*, 269.
(4) Sclafani, A.; Palmisano, L.; Marci, G.; Venezia, A. M. *Sol. Energy Mater. Sol. Cells* **1998**, *51*, 203.
(5) Kohtani, S.; Koshiko, M.; Kudo, A.; Tokumura, K.; Ishigaki, Y.; Toriba, A.; Hayakawa, K.; Nakagaki, R. *Appl. Catal., B* **2003**, *46*, 573.
(6) Mohapatra, S. K.; John, S. E.; Banerjee, S.; Misra, M. *Chem. Mater.* **2009**, *21*, 3048.
(7) Zhang, H. J.; Chen, G. H.; Bahnemann, D. W. *J. Mater. Chem.* **2009**, *19*, 5089.
(8) Zhou, X. M.; Yang, H. C.; Wang, C. X.; Mao, X. B.; Wang, Y. S.; Yang, Y. L.; Liu, G. *J. Phys. Chem. C* **2010**, *114*, 17051.
(9) Ohmori, T.; Takahashi, H.; Mametsuka, H.; Suzuki, E. *Phys. Chem.* **2000**, *2*, 3519.
(10) Aprile, C.; Corma, A.; Garcia, H. *Phys. Chem.* **2008**, *10*, 769.
(11) Rothenberger, G.; Moser, J.; Gratzel, M.; Serpone, N.; Sharma, D. K. *J. Am. Chem. Soc.* **1985**, *107*, 8054.
(12) Rowsell, J. L. C.; Yaghi, O. M. *Microporous Mesoporous Mater.* **2004**, *73*, 3.
(13) Corma, A.; Garcia, H.; Xamena, F. X. L. *Chem. Rev.* **2010**, *110*, 4606.
(14) Farrusseng, D.; Aguado, S.; Pinel, C. *Angew. Chem., Int. Ed.* **2009**, *48*, 7502.
(15) Xamena, F.; Corma, A.; Garcia, H. *J. Phys. Chem. C* **2007**, *111*, 80.
(16) Alvaro, M.; Carbonell, E.; Ferrer, B.; Xamena, F.; Garcia, H. *Chem.—Eur. J.* **2007**, *13*, 5106.
(17) Dan-Hardi, M.; Serre, C.; Frot, T.; Rozes, L.; Maurin, G.; Sanchez, C.; Ferey, G. *J. Am. Chem. Soc.* **2009**, *131*, 10857.
(18) Silva, C. G.; Luz, I.; Llabres i Xamena, F. X.; Corma, A.; Garcia, H. *Chem.—Eur. J.* **2010**, *16*, 11133.
(19) Gascon, J.; Hernandez-Alonso, M. D.; Almeida, A. R.; van Klink, G. P. M.; Kapteijn, F.; Mul, G. *ChemSusChem* **2008**, *1*, 981.
(20) Fu, Y. H.; Sun, D. R.; Chen, Y. J.; Huang, R. K.; Ding, Z. X.; Fu, X. Z.; Li, Z. H. *Angew. Chem., Int. Ed.* **2012**, *51*, 3364.
(21) Horiuchi, Y.; Toyao, T.; Saito, M.; Mochizuki, K.; Iwata, M.; Higashimura, H.; Anpo, M.; Matsuoka, M. *J. Phys. Chem. C* **2012**, *116*, 20848.
(22) Horcajada, P.; Surble, S.; Serre, C.; Hong, D. Y.; Seo, Y. K.; Chang, J. S.; Greneche, J. M.; Margiolaki, I.; Ferey, G. *Chem. Commun.* **2007**, 2820.
(23) Ferey, G.; Mellot-Draznieks, C.; Serre, C.; Millange, F.; Dutour, J.; Surble, S.; Margiolaki, I. *Science* **2005**, *309*, 2040.
(24) Mellot-Draznieks, C.; Serre, C.; Surble, S.; Audebrand, N.; Ferey, G. *J. Am. Chem. Soc.* **2005**, *127*, 16273.
(25) Horcajada, P.; Salles, F.; Wuttke, S.; Devic, T.; Heurtaux, D.; Maurin, G.; Vimont, A.; Daturi, M.; David, O.; Magnier, E.; Stock, N.; Filinchuk, Y.; Popov, D.; Riekel, C.; Ferey, G.; Serre, C. *J. Am. Chem. Soc.* **2011**, *133*, 17839.
(26) Lohe, M. R.; Rose, M.; Kaskel, S. *Chem. Commun.* **2009**, 6056.
(27) Vrubel, H.; Hasegawa, T.; de Oliveira, E.; Nunes, F. S. *Inorg. Chem. Commun.* **2006**, *9*, 208.
(28) Dziobkowski, C. T.; Wrobleski, J. T.; Brown, D. B. *Inorg. Chem.* **1981**, *20*, 671.
(29) Dhakshinamoorthy, A.; Alvaro, M.; Horcajada, P.; Gibson, E.; Vishnuvarthan, M.; Vimont, A.; Greneche, J. M.; Serre, C.; Daturi, M.; Garcia, H. *ACS Catal.* **2012**, *2*, 2060.